




# Improvement of in vitro degradation of magnesium oxychloride cement for bone repair by chitosan

Jing Wen<sup>1</sup>, Jianguo Liao<sup>1,\*</sup> , Qiwei Ying<sup>1</sup>, Hang Li<sup>1</sup>, Yanrui Mao<sup>1</sup>, Suyan Han<sup>1</sup>, and Yu Zhu<sup>1</sup>

<sup>1</sup>Henan Key Laboratory of Materials on Deep-Earth Engineering, School of Materials Science and Engineering, Henan Polytechnic University, Jiaozuo 454000, China

Received: 19 June 2020

Accepted: 21 August 2020

Published online:

14 September 2020

© Springer Science+Business Media, LLC, part of Springer Nature 2020

## ABSTRACT

Ideal inorganic bone cement used for bone repair should have high strength, and the speed of degradation should match the formation rate of new bone tissue. Magnesium oxychloride cement has excellent mechanical properties and non-toxicity to bone marrow stromal cells; however, its application has been hindered by its poor water resistance. In this study, the high-degradation material chitosan (CS) was added to magnesium oxychloride cement (MOC). The compressive strength, mass loss, ion release, and pH value of the composite MOC were analyzed and scanning electron microscopy, energy dispersive spectroscopy, X-ray diffraction, and Fourier transform infrared spectroscopy were conducted. The compressive strength was  $45.4 \pm 5.3$  MPa in cements with 0.5-wt% CS and 2-wt%  $\text{KH}_2\text{PO}_4$  soaked in SBF for 28 d, and the degradation rate reached  $12.67 \pm 0.5\%$ . SEM observations showed good apatite formation of the surfaces of the MOC with 2-wt%  $\text{KH}_2\text{PO}_4$  and with 0.5-wt% CS and 2-wt%  $\text{KH}_2\text{PO}_4$ . The results indicate that the modified MOC possesses good mechanical properties, degradation rate and biological properties. Therefore, it is a promising material for degradable bone filling.

## Introduction

Affording unique and important functions, bone is the largest tissue in the human body. Due to illnesses, accidents or aging, millions of people suffer from bone defects [1]. Bone defect repair has always been a big challenge by surgeons and usually is carried out

by bone transplantation [2]. Currently, autogenous bone grafts and allograft bone transplantation are widely clinically used. Restorative treatment is also used, where the autogenous bone is removed. Consequently, the accepted sites result in pain, inflammation and other side effects. Moreover, allograft bone transplantation always results in immune rejection, viral infections, and slow healing rates.

Handling Editor: Annela M. Seddon.

Address correspondence to E-mail: liaojianguo10@hpu.edu.cn

Furthermore, the collection and restoration are costly and difficult [3]. Thus, the application of artificial bone replacement material is becoming a new treatment. Medical bone cements have many advantages, such as being simple to use and having arbitrary plasticity and self-curing. These can be used for shaping and repair, and thus, they have excellent potential application value [4, 5].

Magnesium oxychloride cement (MOC) is a cementation material made by mixing magnesium oxide (MgO) powder with a magnesium chloride ( $\text{MgCl}_2 \cdot 6\text{H}_2\text{O}$ ) solution [6], which has the advantages of fast solidification and a high early strength [7]. However, its main hydration products,  $3\text{Mg}(\text{OH})_2 \cdot \text{MgCl}_2 \cdot 8\text{H}_2\text{O}$  (phase 3) and  $5\text{Mg}(\text{OH})_2 \cdot \text{MgCl}_2 \cdot 8\text{H}_2\text{O}$  (phase 5), have poor water resistance and are easily decomposed in humid environment [8, 9], resulting in a sharp decline in the compressive strength, which limits the application of MOC in engineering applications [10]. Studies have shown that admixtures, such as phosphoric acid and phosphate, iron salt, copper salt, aluminum salt, organic acids, and polymers, can effectively improve the water resistance of MOC [10–12]. Among these admixtures, the ionized  $\text{H}_2\text{PO}_4^-$ ,  $\text{HPO}_4^{2-}$  and  $\text{PO}_4^{3-}$  produced by phosphoric acid and soluble phosphate in a MOC slurry can reduce the minimum concentration of  $\text{Mg}^{2+}$  in solution required for the formation of the phase 5 or 3 hydration products of MOC and increase the stability of these phases in water, thereby significantly improving the water resistance of MOC [9, 10].

The main elements in MOC,  $\text{Mg}^{2+}$  and  $\text{Cl}^-$ , are essential ions for the human body:  $\text{Mg}^{2+}$  is involved in bone mineral metabolism [13, 14], crystallization and bone formation [15], and  $\text{Cl}^-$  can help maintain the acid–base balance in blood [16]. Therefore, the use of MOC as a medical bone cement with high strength and gradual degradation after modification is proposed in this paper. Previous reports [17] had also shown that MOC is non-cytotoxic and can be used as a biomedical material.

Chitosan (CS) is a product of removing *N*-acetyl chitin, also known as acetyl chitin which can be degraded by enzymes in the body, widely used in the field of tissue engineering [18–20]. CS is insoluble in water and most organic solvents, and it is only soluble in dilute acids, such as dilute acetic acid [21, 22]. Therefore, adding a CS acid solution to the hydration system of MOC will improve its hydration reaction speed. After the reaction, the system will be in a

neutral or slightly alkaline environment, at which point CS will precipitate and cover the surface of the hydration products, blocking their contact with water and improving their water resistance.

In this study, potassium dihydrogen phosphate ( $\text{KH}_2\text{PO}_4$ , referred to as PDP) [23] and CS were used as additives to modify MOC. By adjusting the content of  $\text{KH}_2\text{PO}_4$  and CS, modified MOC with an optimized performance was obtained, and the strength, hardening mechanism, degradation, biological activity, and other properties related to the potential clinical applications of MOC were studied.

## Materials and methods

### Materials

Active magnesium oxide (MgO) was obtained as follows. Magnesium hydroxide ( $\text{Mg}(\text{OH})_2$ , analytically pure, GUANGFU Fine Chemical Industry Research Institute, Tianjin, China) was heated at 700 °C for 3 h in a high-temperature furnace, after which it was removed, rapidly cooled, and ground for later use.

Analytically pure magnesium chloride ( $\text{MgCl}_2 \cdot 6\text{H}_2\text{O}$ ) was obtained from Tianjin Kemiou Chemical Reagent Co., Ltd. Analytically pure PDP ( $\text{KH}_2\text{PO}_4$ ) (content  $\geq 99.5$  wt%) was obtained from the Tianjin Hongyan Reagent Factory. CS with a degree of deacetylation  $\geq 95$  wt% and a viscosity of 100–200 mPa s was obtained from Shanghai Aladdin Bio-Chem Technology Co., Ltd., China. Analytically pure acetic acid ( $\text{CH}_3\text{COOH}$  content  $\geq 99.5\%$ ) was obtained from the Tianjin Fengchuan Chemical Reagent Co., Ltd.

### Preparation of modified MOC

The referenced mixture ratio was  $n(\text{MgO}):n(\text{MgCl}_2):n(\text{H}_2\text{O}) = 13:1:12$ , and 2 wt% PDP was added. This was mixed with the CS powder at specified mass fraction (0.25, 0.5, 0.75, and 1.0) and the specific proportion is shown in Table 1.

The modified MOC preparation process was as follows. Each raw material (CS,  $\text{MgCl}_2$ , PDP, and MgO) was weighed according to a specified proportion. A 5% acetic acid solution in water was prepared. The CS was dissolved in the 5% acetic acid solution to obtain a CS solution.  $\text{MgCl}_2$  was sequentially

**Table 1** Detailed mixture proportions of CS/2-wt% PDP-MOC

	PDP (%)	$n(\text{MgO}):n(\text{MgCl}_2):n(\text{H}_2\text{O})$	CS (wt%)	Liquid phase (aq)
MOC-1	2.0	13:1:12	0	5%CH <sub>3</sub> COOH
MOC-2	2.0	13:1:12	0.25	5%CH <sub>3</sub> COOH
MOC-3	2.0	13:1:12	0.50	5%CH <sub>3</sub> COOH
MOC-4	2.0	13:1:12	0.75	5%CH <sub>3</sub> COOH
MOC-5	2.0	13:1:12	1.00	5%CH <sub>3</sub> COOH

PDP is an abbreviation of KH<sub>2</sub>PO<sub>4</sub>

dissolved in the CS solution and mixed uniformly to obtain a mixed solution B. Finally, MgO powder was added to the B solution and stirred evenly. The mixed material was then filled into cubic molds (10 mm × 10 mm × 10 mm) and cylindrical molds (Ø10 mm × 2 mm). After curing in the air (20 ± 5 °C, humidity 60 ± 5%) for 24 h, the samples were removed from the molds to obtain CS/2-wt% PDP-MOC samples for subsequent characterization.

## Characterization methods

### Compressive strength

The modified MOC samples (dimensions of 10 mm × 10 mm × 10 mm, six samples in each group) were polished and tested by general testing machine (CMT-20, Jinan Liangong Testing Technology Co., Ltd.) to measure compressive strength. Another set of samples (six samples per group) was placed in a polyethylene tube and immersed in simulated body fluid (SBF, prepared from references [24]). The volume ratio of the sample to the soaking solution was 1:10. The polyethylene tube was stored in a constant temperature oscillating water bath (37.5 °C, oscillation frequency: 72 rpm). The solution was refreshed every 3 d. The samples were removed from the SBF after 3, 7, 14, 21, and 28 d and washed with distilled water three times. The universal testing machine was used to test the soaking sample compressive strengths, and the crosshead speed was set at 0.5 mm min<sup>-1</sup>.

### Mass loss rate

The demolded modified MOC (Ø10 mm × 2 mm) samples were washed with absolute ethanol, dried in an oven at 60 °C for 5 h, and weighed. This weight was recorded as M<sub>0</sub>. The sample was then set in a polyethylene tube, and the ratio of the SBF solution to the cylindrical sample surface (Ø10 mm × 2 mm)

was 10 mL/cm<sup>2</sup>. The solution was refreshed every 3 d.

After immersion for 3, 7, 14, 21, and 28 d, the sample (Ø10 mm × 2 mm) was removed and dried. The sample was then weighed, and the weight was recorded as M<sub>t</sub>. The mass loss rate of the sample (ML) was calculated as follows:  $ML = (M_0 - M_t) / M_0 \times 100\%$ .

### The change of pH value

A set of samples (Ø10 mm × 2 mm) were soaked in SBF for 24, 48, 72, 96, 120, 144, and 168 h, and the SBF solution was replaced after each 24 h. The pH instrument (PHS-3C, Shanghai Jason, Instrument, China) was used to test the pH value.

### In vitro ion concentration

The CS/2-wt% PDP-MOC cement samples were immersed in SBF ( $V_{\text{MOC}}:V_{\text{SBF}} = 1:20$ ) without replacing the SBF solution. After soaking in SBF for 1, 2, 3, 5 and 7 d, the samples were removed from the solution and the concentrations of Ca<sup>2+</sup>, Mg<sup>2+</sup> and Cl<sup>-</sup> in the SBF solution were tested by an Automatic Potentiometric Titrator (T960 Potentiometric Titrator, Calcium Composite Electrode, Silver Composite Electrode, Shandong Haineng Instrument, China).

### Surface crystal structure and morphology test

After the specified period, the samples were removed from the SBF, washed with distilled water, dried, and analyzed by infrared spectroscopy (Fourier transform infrared spectrometer, PerkinElmer, USA) to analyze the surface group compositions. The crystal phase structure of the surface layer was determined using a rotating target X-ray powder polycrystal diffractometer (Rigaku, Japan; operating conditions: 9 kW, CuK $\alpha$  radiation source,  $\lambda = 0.154$  nm, scanning range

10°–80°). The morphological features of the cements before and after immersion in SBF were examined using field-emission scanning electron microscopy (FE-SEM, JSM-6390LV, JEOL, Japan). The samples were sputter-coated with gold prior to examination.

## Results

### Mechanical property

Figure 1 shows the compressive strength of composite modified MOC (37.5 °C, humidity 60%, and hardening 24 h) samples after immersion in SBF for 3, 7, 14, 21, and 28 d. The results indicated that the compressive strength of the cement decreased with the increasing amount of CS. The cements with 0.5 wt% CS may have reached the maximum value. When immersed in SBF, the strength of the cement decreased slowly as a function of immersion time. Furthermore, the strength of the cement with 0.5 wt% CS was the highest of all the groups of every immersion time, and the strength after 28 d was  $45.4 \pm 5.3$  MPa.

### In vitro degradation of MOC

The mass loss rates of the cements with different CS contents are shown in Fig. 2. As shown in Fig. 2, the mass loss rate of the cement increased more gradually with longer immersion times and the increase in the CS content. A rapid increase in the first 7 days was followed by a much slow increase. The mass loss

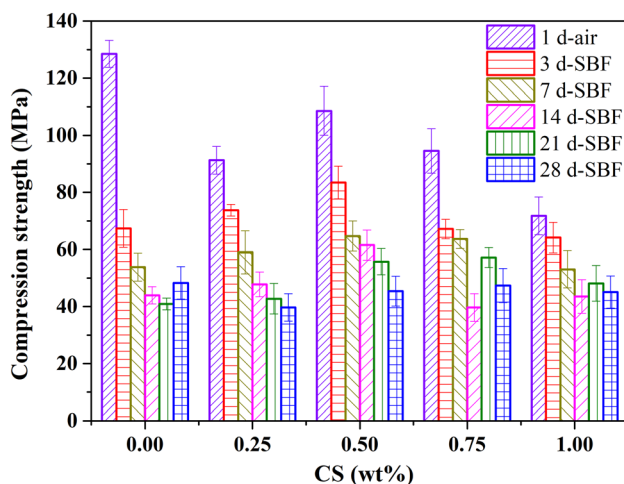


**Figure 1** Compressive strength of CS/2-wt% PDP-MOC in SBF (37.5 °C) after immersion times.

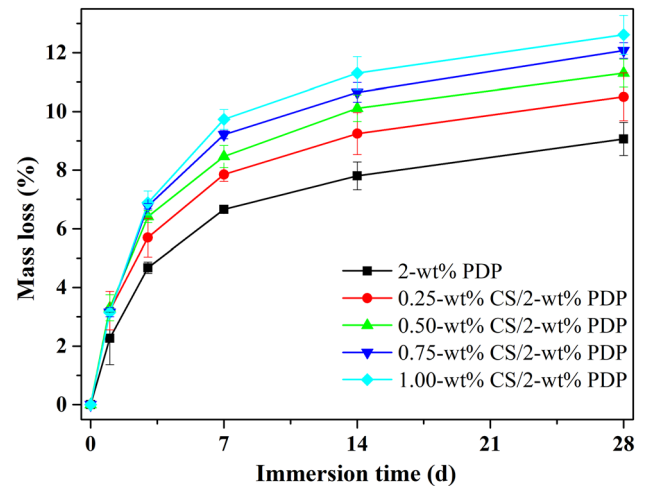


**Figure 2** Mass loss rate of CS/2-wt% PDP-MOC after soaking in SBF (37.5 °C).

rate of the 1.0-wt% CS/2-wt% PDP-MOC reached  $11.3 \pm 0.6\%$ , while those of the 0.5-wt% CS/2-wt% PDP-MOC and 2-wt% PDP-MOC reached only  $10.1 \pm 0.5\%$  and  $7.8 \pm 0.5\%$ , respectively, after being immersed for 14 d. After immersion in SBF for 28 d, the mass loss of the 0.5-wt% CS/2-wt% PDP-MOC reached  $12.7 \pm 0.5\%$ . These results implied that the doping of CS improved the degradability of the composite cements. The samples tended to completely degrade, which may be beneficial for the repair of human bones.

The pH value change from the SBF solutions after immersion in the cements for different times are shown in Fig. 3. The pH value increased from the starting value of 7.2 to 9.6–10.3 within 24 h. With the extension of the soaking time, the pH value of the MOC was maintained between 8.7 and 9.0. The pH value of the cement decreased more gradually with the increase in the CS content, indicating that the addition of CS may prevent the hydrolysis of MgO and phase 5 to a certain extent.

Figure 4 shows the changes in the ion concentrations of SBF after the immersion of the CS/2% PDP-MOC for different times. The  $Mg^{2+}$  and  $Cl^{-}$  ion concentrations continued to increase, while the  $Ca^{2+}$  ion concentrations decreased with time and with the increase in the CS content. These results are consistent with the mass loss rate results shown in Fig. 2. The release of  $Ca^{2+}$  ions was found to be higher for the 2-wt% PDP-MOC, followed by that for the CS/2-wt% PDP-MOC.  $Ca^{2+}$  ions in the solution deposited to form apatite on the material surfaces.

**Figure 3** pH change of CS/2-wt% PDP-MOC after different soaking times.

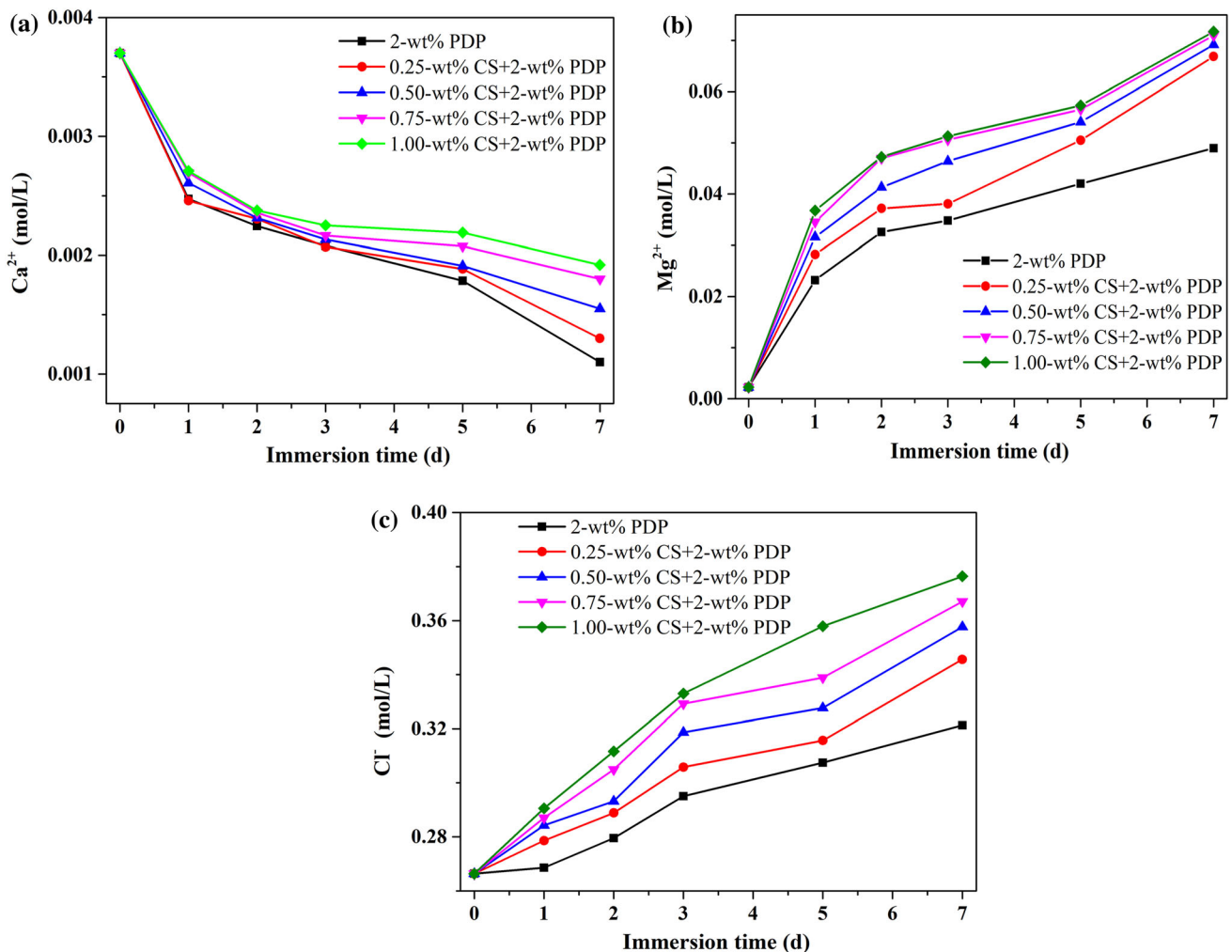
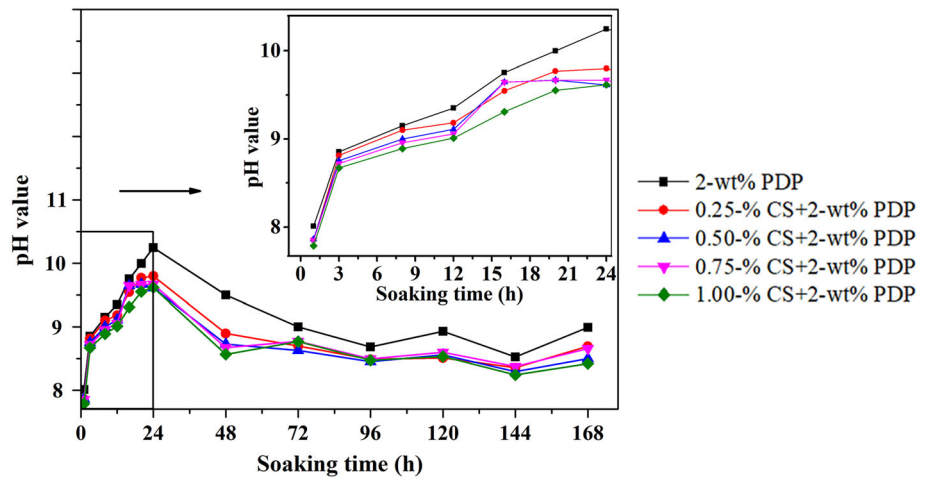


**Figure 4** Changes in  $\text{Ca}^{2+}$ ,  $\text{Mg}^{2+}$ , and  $\text{Cl}^-$  concentrations (mol/L) in SBF solution: **a**  $\text{Ca}^{2+}$ , **b**  $\text{Mg}^{2+}$ , and **c**  $\text{Cl}^-$ .

Figure 5a, b shows XRD patterns of the 2-wt% PDP-MOC and the 0.5-wt% CS/2-wt% PDP-MOC, respectively, after soaking in SBF for 3, 7, 14, and 28

d. Due to the larger molar ratio of active  $\text{MgO}/\text{MgCl}_2$  (equal to 13), the main crystal phases of MOC were  $\text{MgO}$  and phase 5. After immersion in SBF, a new



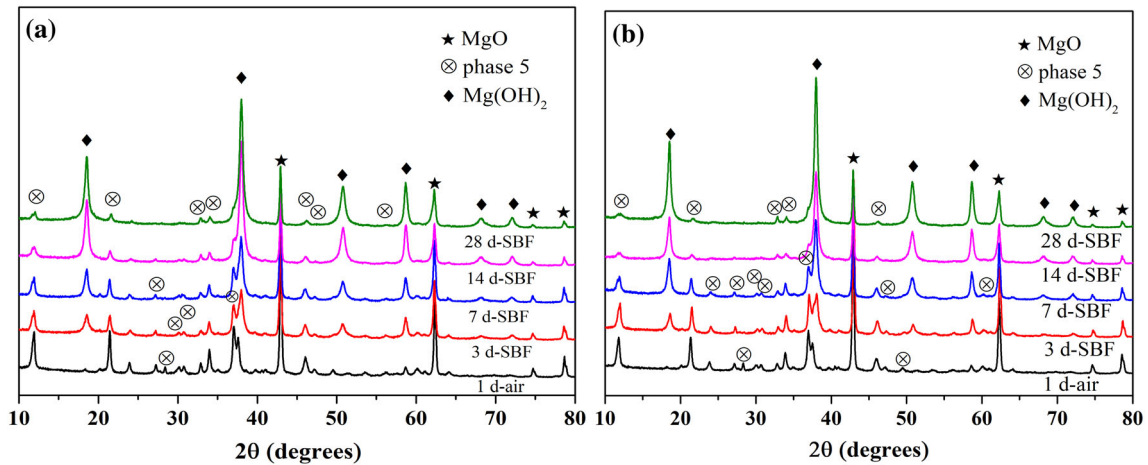


**Figure 5** XRD patterns of MOC powders in air ( $20 \pm 5^\circ\text{C}$ ,  $60 \pm 5\%$  relative humidity) for 1 d and SBF solution for different times: **a** 2-wt% PDP-MOC and **b** 0.5-wt% CS/2-wt% PDP-MOC.

phase  $\text{Mg}(\text{OH})_2$  formed. With increasing immersion time, the phase 5 and MgO contents decreased and the  $\text{Mg}(\text{OH})_2$  content increased.

### In vitro bioactivity of MOC

The FTIR spectra of the sample surface of the MOC immersed in the SBF solution for different times are shown in Fig. 6. After immersion in SBF, the spectra of the cement showed major peaks associated with HA, such as the peak at  $\sim 1034\text{ cm}^{-1}$  corresponding to the  $\text{PO}_4^{3-}$   $\nu_3$  resonance and the peak at  $\sim 565\text{ cm}^{-1}$  corresponding to the  $\text{PO}_4^{3-}$   $\nu_4$  resonance [1, 25, 26]. These two peaks became more intense with longer immersion times, and the peak intensity of  $\text{PO}_4^{3-}$  of the 0.5-wt% CS/2-wt% PDP-

MOC is significantly higher than that of 2-wt% PDP-MOC. Peaks corresponding to the  $\text{CO}_3^{2-}$   $\nu_3$  vibrations at  $\sim 1430\text{ cm}^{-1}$  were present in the spectra for the samples after immersion, revealing the formation of a carbonate-substituted HA product [27]. The formation of carbonate-substituted HA presumably resulted from the presence of dissolved  $\text{CO}_2$  in the SBF.

Figure 7a, b shows the XRD patterns of the surface of the 2-wt% PDP-MOC and the 0.5-wt% CS/2-wt% PDP-MOC, respectively, after immersion in SBF for 3, 7, 14, and 28 d. XRD showed that the main crystal phases on the surface of the modified MOC after soaking in SBF were unreacted MgO and phase 5. There were some differences between the unsoaked and soaked samples. With the increase in the soaking

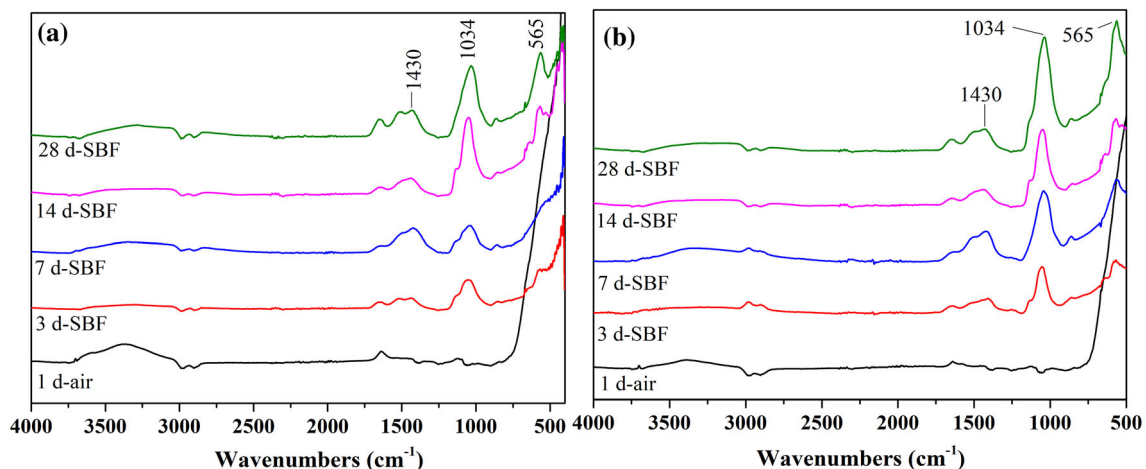


**Figure 6** FTIR spectra of the surfaces of the modified MOC samples that were immersed in air ( $20 \pm 5^\circ\text{C}$ ,  $60 \pm 5\%$  relative humidity) for 1 d and SBF after different periods: **a** 2-wt% PDP-MOC and **b** 0.5-wt% CS/2-wt% PDP-MOC.

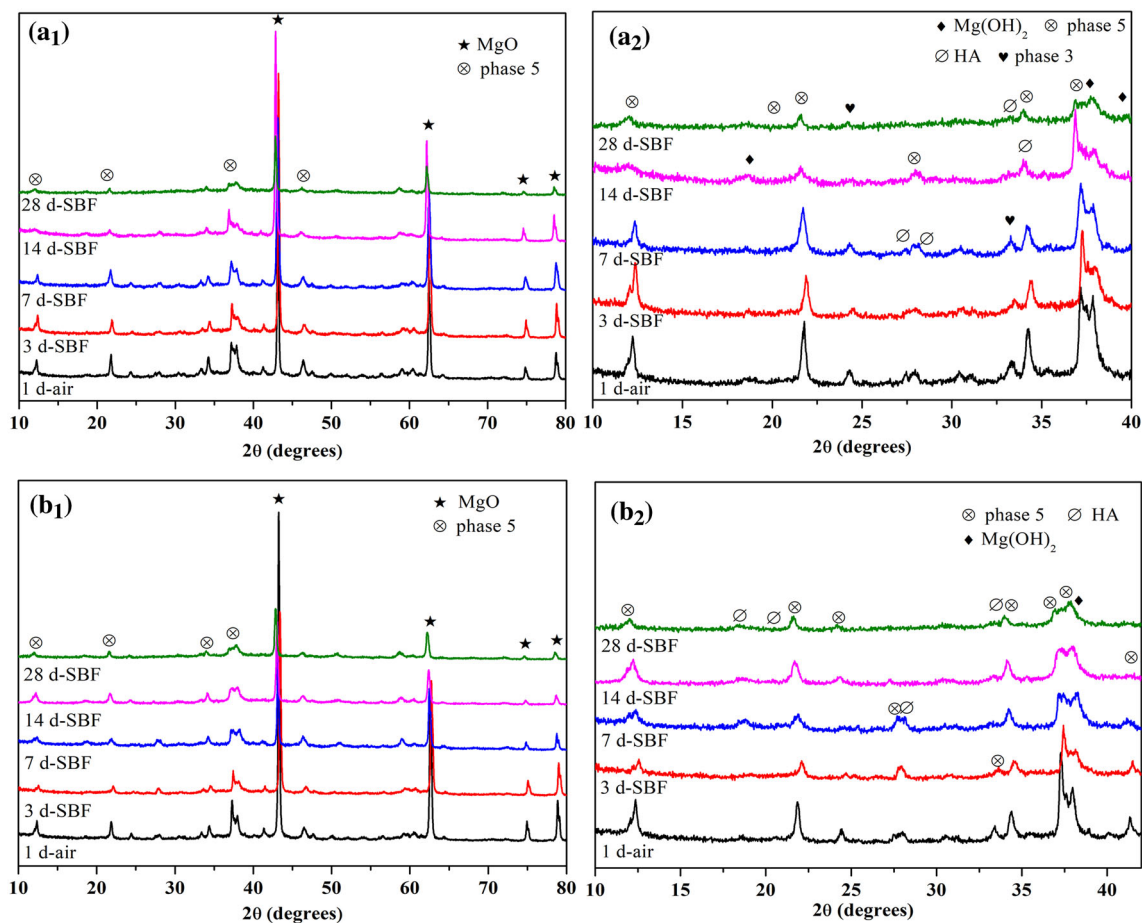


**Figure 7** XRD pattern of the surfaces of the MOC samples in the air ( $20 \pm 5$  °C,  $60 \pm 5\%$  relative humidity) for 1 d and SBF after different periods: **a<sub>1</sub>**, **a<sub>2</sub>** 2-wt% PDP-MOC and **b<sub>1</sub>**, **b<sub>2</sub>** 0.5-wt% CS/2-wt% PDP-MOC.

time, the peaks of the phase 5 and MgO became weaker, and diffraction peaks of HA began to appear.

SEM images of the surface of the cement with 2-wt% PDP and 0.5-wt% CS/2-wt% PDP as-prepared and after immersion in SBF solution for 3, 7, 14, and 28 d are shown in Fig. 8. The as-prepared cements with 2-wt% PDP showed a rough surface with many slender needle-like structures (Fig. 8a<sub>0</sub>), while the cements with 0.5-wt% CS/2-wt% PDP were covered with columns and spherical particles (Fig. 8a<sub>1</sub>). After immersion in the SBF solution for 3 and 7 d, the acicular structure on the surface of 2-wt% PDP-MOC disappeared, and more pores were visible (Fig. 8a<sub>1</sub>, a<sub>2</sub>). The surface structure was loose, and many cracks appeared (Fig. 8a<sub>3</sub>) in the sample immersed in the SBF solution for 14 d. The surface of the 0.5-wt% CS/2-wt% PDP-MOC formed plate-like Mg(OH)<sub>2</sub> after 3 d (Fig. 8b<sub>1</sub>), and spheres appeared on the surface (Fig. 8b<sub>2</sub>) for 7 d.

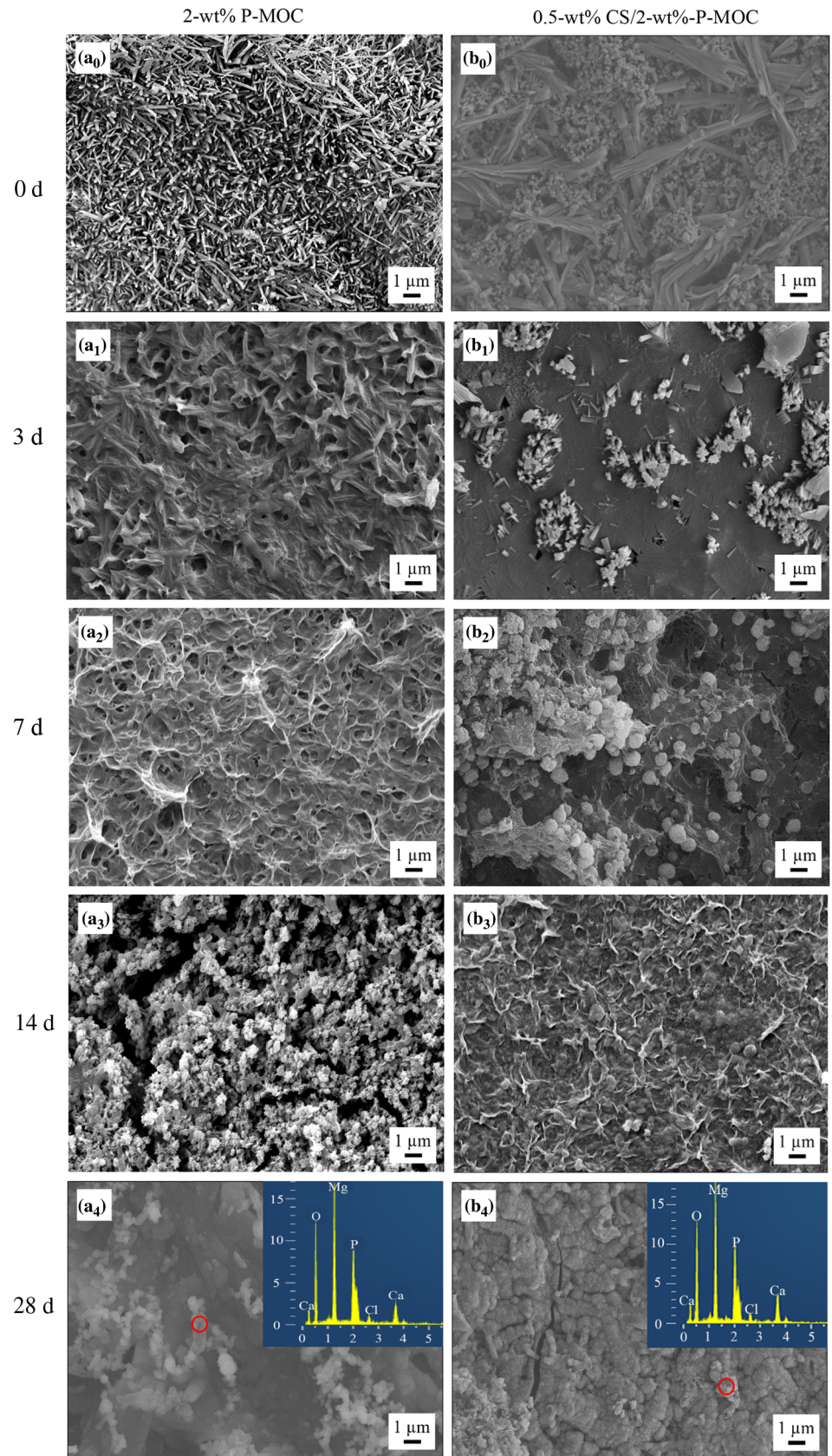
The presence of 0.5-wt% CS resulted in smaller voids compared to the cements without CS. Furthermore, the structures of the cements with 0.5-wt% CS/2-wt% PDP were denser, which could improve the cement strength and water resistance. In addition, there were spheroids on both surfaces when immersed for 28 d. A uniform distribution of Mg along with other elements, such as Ca, P and O, in the cement sample was confirmed by the EDS mapping, and it can be inferred that the spheroids were HA.

## Discussion

The mechanical properties, especially the compressive strength and elastic modulus, are key factors to determine whether bone materials can be applied in the human body [28]. The compressive strength of human cancellous bone is approximately 2–45 MPa, and the compressive strength of cortical bone is

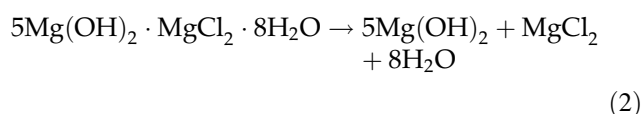
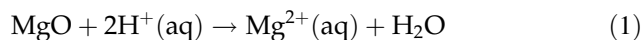


**Figure 8** SEM images of the cements with **a** 2-wt% PDP and **b** 0.5-wt% CS/2-wt% PDP: **a<sub>0</sub>**, **b<sub>0</sub>** as-prepared and **a<sub>1</sub>–a<sub>4</sub>**, **b<sub>1</sub>–b<sub>4</sub>** after immersion in SBF.





approximately 90–230 MPa. The compressive strength of inorganic bone cement for clinical application is generally between those of cancellous and cortical bone [26–29]. Figure 1 shows the compressive strength of the CS/2-wt% PDP-MOC. The compressive strength of the 0.5-wt% CS/2-wt% PDP-MOC was approximately  $45.4 \pm 5.3$  MPa after being soaked in SBF for 28 d, and the strength met the requirements of bone cement. The main reason for the degradation of MOC's mechanical properties in aqueous solution is the instability of its main crystalline phase (phase 5) in water, which is easily eroded by water to reduce its strength [30, 31]. Meanwhile, the initial unreacted MgO reacts with water to form  $\text{Mg}(\text{OH})_2$ , which will also destroy the structure of the MOC. From the XRD results shown in Fig. 8, the characteristic peaks of  $\text{Mg}(\text{OH})_2$  were generated with longer water immersion, and the contents of phase 5 and MgO gradually decreased. The hydrolysis of phase 5 and the reaction between MgO and  $\text{H}^+$  can be described by the following reaction equation [10, 32].



MOC is a low alkalinity cement in which the main hydration product (phase 5) exists stably in a pH range of 9–10.37 [6, 33]. The pH value of MOC is mainly determined by  $\text{Mg}(\text{OH})_2$ . When MgO is mixed with a  $\text{MgCl}_2$  solution, the compound  $\text{Mg}(\text{OH})_2$  will form. In the early stage of hydration, MgO reacts with  $\text{H}^+$  to form  $\text{Mg}(\text{OH})_2$  in the high-concentration  $\text{MgCl}_2$  solution (where the  $\text{H}_2\text{O}/\text{MgCl}_2$  molar ratio is less than 20, and the density is greater than  $1.16 \text{ g/cm}^3$ ) [34]. In addition, the phase 5 decomposition of the MOC surface to form  $\text{Mg}(\text{OH})_2$  will also cause a rapid rise in the pH value. Figure 3 shows that the pH value of the MOC with CS was slightly lower than the pH of the MOC without the CS, which could be attributed to the CS having weakly basic  $-\text{NH}_2$  groups [27]. This reduced the pH inside the MOC system to some extent. After 2 d of immersion, the pH value was maintained at 8.25–8.75. This result indicated that the rapid decline of the pH value did not continue but remained within a small range. In fact, SBF is not a buffer system. If this material was used as an implant, initial contact

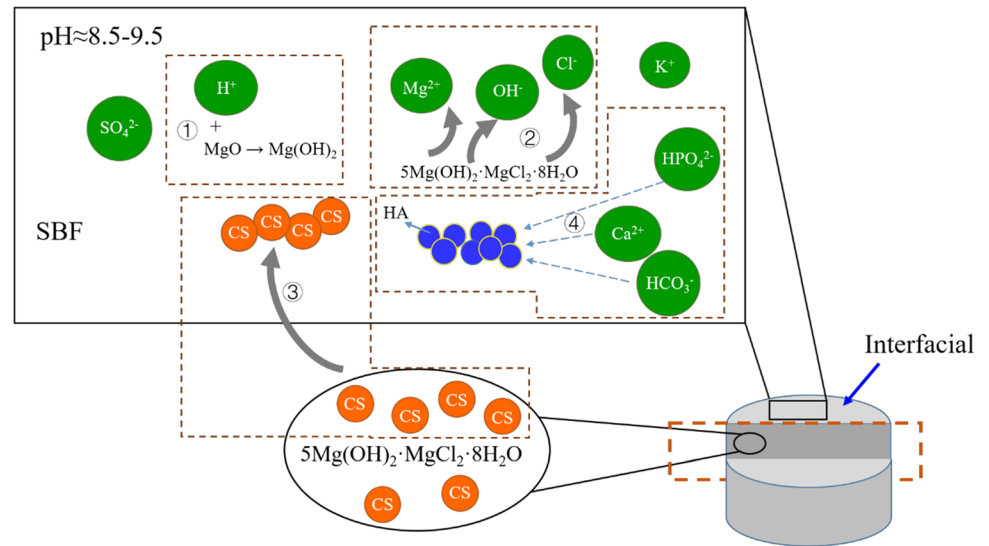
with liquid buffering connective tissue might help to significantly reduce the initial pH value [35]. Therefore, the pH value in Fig. 3 will not have a significant impact on the human body. It was reported that an alkaline environment is favorable for the formation of apatite [36]. The nucleation rate of hydroxyapatite crystals is faster at a pH of 9 than at a pH of 7 [37]. This could also explain why the concentration of  $\text{Ca}^{2+}$  after 2-wt% PDP-MOC immersion was lower than that of the 0.5-wt% CS/2-wt% PDP-MOC immersion (Fig. 4).

In general, the ionic changes produce pH value variations in physiological conditions [38]. In the MOC slurry, PDP is decomposed into various phosphate anions, such as  $\text{H}_2\text{PO}_4^-$ ,  $\text{HPO}_4^{2-}$ ,  $\text{PO}_4^{3-}$ , and  $\text{H}^+$ . Meanwhile, these phosphate anions may be combined with certain ions and aggregate near MgO particles, forming some colloidal materials in situ, which inhibits the early reaction of MgO and prolongs the induction period, delays the speed of subsequent MgO reactions. The presence of phosphate anions significantly reduced the solubility of phase 5 and improved the stability of phase 5 in water [34]. When 2-wt% PDP/0.5-wt% CS was added, the SEM image in Fig. 9 shows that the surface structure of the MOC was compact after soaking, which should have been related to the sol-gel transition as the pH value of the CS solution increased above  $\sim 6.5$  [26]. In addition, CS is insoluble in water, and it will precipitate in an alkaline environment, from a polymer film on the surface of the cement, hinder contact with the water, and improve the stability of the cement.

The ability of biomaterials to form chemical bonds with living bone tissue is related to the apatite mineralization rate [39]. In general, the biological activities of biomaterials can be evaluated by soaking in an in vitro SBF solution through the formation of bone-like apatite layers on the surface [40, 41].

If spherical HA is formed after the material is soaked in a simulated body fluid, the  $\text{Ca}^{2+}$  concentration of the SBF solution will decrease. This is confirmed by the  $\text{Ca}^{2+}$  concentration change in Fig. 4 and the formation of HA in Fig. 8. After CS was added, the concentration of  $\text{Mg}^{2+}$  and  $\text{Cl}^-$  in the solution increased after the MOC was soaked in SBF, indicating that the addition of CS was beneficial to the degradation of MOC. Degradation of bone cement can form a new bone growth space in the body, but the excessively fast degradation rate does not match the growth rate of new bone [28]; how to

**Figure 9** The precipitation process of apatite on MOC.



adjust the degradation of materials to match the rate of new bone formation is an important science question [42].

As shown in Fig. 7, the characteristic peaks of apatite appeared in the XRD patterns of the 2-wt% PDP-MOC and 0.5-wt% CS/2-wt% PDP-MOC, indicating that apatite formed on the cement surface, which confirmed the biological activity of the material. CS has excellent metal-binding capabilities [26]. The amine groups in the CS molecules were responsible for the uptake of metal cations ( $\text{M}^{n+}$ ) by chelation [43]. Metal ions, acting as the acid, constituted acceptors of electron pairs donated by chitosan, acting as the base [44]. This facilitated precipitation of apatite on the cement surface [26, 44]. The precipitation process of apatite on MOC is shown in Fig. 9. The dissolution of MOC occurred in the SBF initially, and rapid ion exchange occurred between the  $\text{M}^{n+}$  ions from the SBF and the  $\text{Mg}^{2+}$  ions from the MOC surface. Because the MgO content in the MOC was excessive,  $\text{Mg}^{2+}$  dissolved from the surface of the MOC could be quickly dissolved into SBF;  $\text{Mg}^{2+}$  has also been shown to facilitate the formation of metastable calcium phosphate salts and control apatite formation [16].  $\text{Mg}^{2+}$  acted as nucleation centers. In addition, the phases 5 on the MOC decomposed into  $\text{Mg}^{2+}$ ,  $\text{Cl}^-$ , and  $\text{OH}^-$ , which caused an increase in the solution pH value, and the CS dissolved in the MOC underwent a sol-gel reaction and precipitated out of the MOC. With increased immersion time in SBF,  $\text{Ca}^{2+}$ ,  $\text{Mg}^{2+}$ ,  $\text{PO}_4^{3-}$ , and  $\text{CO}_3^{2-}$  in the SBF were

deposited on the MOC surface in large quantities, and apatite gradually formed.

## Conclusion

In this study, the effect of CS and PDP on the properties of MOC was investigated. The findings obtained from this study are summarized as follows:

1. When the MOC with 0.5-wt% CS/2-wt% PDP was soaked in SBF for 28 d, the strength reached  $45.4 \pm 5.3$  MPa, and the mass loss rate increased slowly from  $7.20 \pm 0.4\%$  at 14 d to  $12.67 \pm 0.5\%$  at 28 d.
2. The addition of CS decreased the pH value of the MOC system to a certain extent, and the addition of 0.5-wt% CS/2-wt% PDP could make the structure of surface of the MOC denser and improve the stability of the cement.
3. Hydroxyapatite appeared on the surface of the modified MOC, indicating that the MOC had a certain biological activity.

In summary, modified MOC with high mechanical and appropriate degradation rate and biological properties would potentially be a promising choice for degradable bone filling materials.

## Acknowledgements

This work was financially supported by the Fundamental Research Funds for the Universities of Henan

Province (Grant No. NSFRF180311), the Education Department of Henan Province Basic Research Program, China (Grant Nos. 19A430015, 19B430004).

### Compliance with ethical standards

**Conflict of interest** The authors declare that they have no conflict of interest.

### References

- [1] Hemmati K, Hesaraki S, Nemati A (2014) Evaluation of ascorbic acid-loaded calcium phosphate bone cements: physical properties and in vitro release behavior. *Ceram Int* 40:3961–3968
- [2] Yang F, Zhou L, Liu B, Luo Z (2013) Current status and prospect of artificial bone repair materials. *Int Conf Biol Environ Chem* 58:82–85
- [3] Marzec M, Kucinska-Lipka J, Kalaszczynska I, Janik H (2017) Development of polyurethanes for bone repair. *Mater Sci Eng C Mater Biol Appl* 80:736–747
- [4] Wang Y, Wei J, Guo H, Liu C (2006) Bioactive calcium phosphate cement with anti-washout for bone replacement. *J Inorg Mater* 21:1435–1442 **(in Chinese)**
- [5] O’Neill R, McCarthy HO, Montufar EB, Ginebra MP, Wilson DI, Lennon A et al (2017) Critical review: injectability of calcium phosphate pastes and cements. *Acta Biomater* 50:1–19
- [6] Ba H, Guan H (2009) Influence of MgO/MgCl<sub>2</sub> molar ratio on phase stability of magnesium oxychloride cement. *J Wuhan Univ Technol* 24:476–481
- [7] Góchez R, Wambaugh J, Rochner B, Kitchens CL (2017) Kinetic study of the magnesium oxychloride cement cure reaction. *J Mater Sci* 52:7637–7646. <https://doi.org/10.1007/s10853-017-1013-x>
- [8] He P, Poon CS, Tsang DCW (2017) Using incinerated sewage sludge ash to improve the water resistance of magnesium oxychloride cement (MOC). *Constr Build Mater* 147:519–524
- [9] Góchez R, Vreeland T, Wambaugh J, Kitchens CL (2017) Conversion of magnesium oxychloride to chlorartinite and resulting increased water resistance. *Mater Lett* 207:1–3
- [10] Deng D (2003) The mechanism for soluble phosphates to improve the water resistance of magnesium oxychloride cement. *Cem Concr Res* 33:1311–1317
- [11] Zhang C, Deng D (1995) The effect of aluminate minerals on magnesium oxychloride cement. *J Chin Ceram Soc* 23:211–218 **(in Chinese)**
- [12] He P, Poon CS, Tsang DCW (2017) Effect of pulverized fuel ash and CO<sub>2</sub> curing on the water resistance of magnesium oxychloride cement (MOC). *Cem Concr Res* 97:115–122
- [13] Tamimi F, Nihouannen DL, Bassett DC, Ibasco S, Gbureck U, Knowles J et al (2011) Biocompatibility of magnesium phosphate minerals and their stability under physiological conditions. *Acta Biomater* 7:2678–2685
- [14] Cabrejos-Azama J, Alkhraisat MH, Rueda C, Torres J, Blanco L, López-Cabarcos E (2014) Magnesium substitution in brushite cements for enhanced bone tissue regeneration. *Mater Sci Eng C Mater Biol Appl* 43:403–410
- [15] Ding Z, Li H, Wei J, Li R, Yan Y (2018) Developing a novel magnesium glycerophosphate/silicate-based organic-inorganic composite cement for bone repair. *Mater Sci Eng C Mater Biol Appl* 87:104–111
- [16] Tan Y, Liu Y, Zhao Z, Paxton JZ, Grover LM (2015) Synthesis and in vitro degradation of a novel magnesium oxychloride cement. *J Biomed Mater Res A* 103:194–202
- [17] Tan Y (2011) Development and characterization of orthopedic filling materials (Doctor). Central South University **(in Chinese)**
- [18] Barros AA, Alves A, Nunes C, Coimbra MA, Pires RA, Reis RL (2013) Carboxymethylation of ulvan and chitosan and their use as polymeric components of bone cements. *Acta Biomater* 9:9086–9097
- [19] Younes I, Rinaudo M (2015) Chitin and chitosan preparation from marine sources. Structure, properties and applications. *Mar Drugs* 13:1133–1174
- [20] Anitha A, Sowmya S, Kumar PTS, Deepthi S, Chennazhi KP, Ehrlich H et al (2014) Chitin and chitosan in selected biomedical applications. *Prog Polym Sci* 39:1644–1667
- [21] Dragostin OM, Samal SK, Dash M, Lupascu F, Pânzariu A, Tuchilus C et al (2016) New antimicrobial chitosan derivatives for wound dressing applications. *Carbohydr Polym* 141:28–40
- [22] Jayakumar R, Prabakaran M, Sudheesh Kumar PT, Nair SV, Tamura H (2011) Biomaterials based on chitin and chitosan in wound dressing applications. *Biotechnol Adv* 29:322–337
- [23] He P, Poon CS, Tsang DCW (2018) Comparison of glass powder and pulverized fuel ash for improving the water resistance of magnesium oxychloride cement. *Cem Concr Compos* 86:98–109
- [24] Kokubo T, Takadama H (2006) How useful is SBF in predicting in vivo bone bioactivity? *Biomaterials* 27:2907–2915
- [25] Li H, Wang D, Wu Y, Yao A, Ye S (2017) Effect of citric acid concentration on the properties of borate glass bone cement. *J Inorg Mater* 32:831–836 **(in Chinese)**
- [26] Cui X, Zhang Y, Wang H, Gu Y, Li L, Zhou J et al (2016) An injectable borate bioactive glass cement for bone repair:

- preparation, bioactivity and setting mechanism. *J Non Cryst Solids* 432:150–157
- [27] Cui X, Huang W, Zhang Y, Huang C, Yu Z, Wang L et al (2017) Evaluation of an injectable bioactive borate glass cement to heal bone defects in a rabbit femoral condyle model. *Mater Sci Eng C Mater Biol Appl* 73:585–595
- [28] Tang Y, Chen L, Wu Z, Zhao K, Tan Q (2017) Fabrication of injectable and expandable PMMA/PAAS f bone cements. *Compos Sci Technol* 146:203–209
- [29] Perumal G, Ramasamy B, Nandkumar AM, Doble M (2018) Influence of magnesium particles and pluronic F127 on compressive strength and cytocompatibility of nanocomposite injectable and moldable beads for bone regeneration. *J Mech Behav Biomed Mater* 88:453–462
- [30] Wen J, Yu H, Li Y, Wu C, Dong J, Zheng L (2013) Effects of  $H_3PO_4$  and  $Ca(H_2PO_4)_2$  on mechanical properties and water resistance of thermally decomposed magnesium oxychloride cement. *J Cent South Univ* 20:3729–3735
- [31] Tan Y, Liu Y, Grover L (2014) Effect of phosphoric acid on the properties of magnesium oxychloride cement as a bio-material. *Cem Concr Res* 56:69–74
- [32] Sglavo VM, De Genua F, Conci A, Ceccato R, Cavallini R (2011) Influence of curing temperature on the evolution of magnesium oxychloride cement. *J Mater Sci* 46:6726–6733. <https://doi.org/10.1007/s10853-011-5628-z>
- [33] Wei L, Wang Y, Yu J, Xiao J, Xu S (2018) Feasibility study of strain hardening magnesium oxychloride cement-based composites. *Constr Build Mater* 165:750–760
- [34] Huang T, Yuan Q, Deng D (2019) The role of phosphoric acid in improving the strength of magnesium oxychloride cement pastes with large molar ratios of  $H_2O/MgCl_2$ . *Cem Concr Compos* 97:379–386
- [35] Lee HJ, Kim B, Padalhin AR, Lee BT (2019) Incorporation of chitosan-alginate complex into injectable calcium phosphate cement system as a bone graft material. *Mater Sci Eng C Mater Biol Appl* 94:385–392
- [36] Le HR, Chen KY, Wang CA (2012) Effect of pH and temperature on the morphology and phases of co-precipitated hydroxyapatite. *J Sol–Gel Sci Technol* 61:592–599
- [37] Yang G, Liu J, Li F, Pan Z, Ni X, Shen Y et al (2014) Bioactive calcium sulfate/magnesium phosphate cement for bone substitute applications. *Mater Sci Eng C Mater Biol Appl* 35:70–76
- [38] Miller MA, Kendall MR, Jain MK, Larson PR, Madden AS, Tas AC (2012) Testing of brushite ( $CaHPO_4 \cdot 2H_2O$ ) in synthetic biomineralization solutions and in situ crystallization of brushite micro-granules. *J Am Ceram Soc* 95:2178–2188
- [39] Chen Z, Li X, He H, Ren Z, Liu Y, Wang J et al (2012) Mesoporous silica nanoparticles with manipulated microstructures for drug delivery. *Colloids Surf B* 95:274–278
- [40] Ruan Z, Yao D, Xu Q, Liu L, Tian Z, Zhu Y (2017) Effects of mesoporous bioglass on physicochemical and biological properties of calcium sulfate bone cements. *Appl Mater Today* 9:612–621
- [41] Wu M, Wang T, Wang Y, Wang H (2019) Ultrafast bone-like apatite formation on bioactive tricalcium silicate cement using mussel-inspired polydopamine. *Ceram Int* 45:3033–3043
- [42] Zhou X, Qian Y (2015) Stability of tissue engineering bone in the repair of bone defects: material degradation and bone formation. *Chin J Tissue Eng Res* 19:1938–1942 (**in Chinese**)
- [43] Wawro D, Pighinelli L (2011) Chitosan fibers modified with HAp/ $\beta$ -TCP nanoparticles. *Int J Mol Sci* 12:7286–7300
- [44] Czechowska J, Zima A, Paszkiewicz Z, Lis J, Ślósarczyk A (2014) Physicochemical properties and biomimetic behaviour of  $\alpha$ -TCP-chitosan based materials. *Ceram Int* 40:5523–5532

**Publisher's Note** Springer Nature remains neutral with regard to jurisdictional claims in published maps and institutional affiliations.